



Discovery of small molecule isozyme non-specific inhibitors of mammalian acetyl-CoA carboxylase 1 and 2

Jeffrey W. Corbett^{a,*}, Kevin D. Freeman-Cook^a, Richard Elliott^a, Felix Vajdos^a, Francis Rajamohan^a, Darcy Kohls^a, Eric Marr^a, Hailong Zhang^b, Liang Tong^b, Meihua Tu^a, Sharad Murdande^a, Shawn D. Doran^a, Janet A. Houser^a, Wei Song^a, Christopher J. Jones^a, Steven B. Coffey^a, Leanne Buzon^a, Martha L. Minich^a, Kenneth J. Dirico^a, Susan Tapley^a, R. Kirk McPherson^a, Eliot Sugarman^a, H. James Harwood Jr.^a, William Esler^a

^a Pfizer Global Research and Development, Eastern Point Road, Groton, CT 06340, USA

^b Columbia University, New York, NY 10027, USA

ARTICLE INFO

Article history:

Received 21 January 2009

Revised 19 April 2009

Accepted 21 April 2009

Available online 24 April 2009

Keywords:

Acetyl-CoA carboxylase

ACC

Enzyme inhibitor

Spirochromanone

ACC1

ACC2

Structure based drug discovery

Diabetes

Metabolic syndrome

ABSTRACT

Screening Pfizer's compound library resulted in the identification of weak acetyl-CoA carboxylase inhibitors, from which were obtained rACC1 CT-domain co-crystal structures. Utilizing HTS hits and structure-based drug discovery, a more rigid inhibitor was designed and led to the discovery of sub-micromolar, spirochromanone non-specific ACC inhibitors. Low nanomolar, non-specific ACC-isozyme inhibitors that exhibited good rat pharmacokinetics were obtained from this chemotype.

© 2010 Elsevier Ltd. All rights reserved.

Type-2 diabetes mellitus (T2DM) has reached epidemic proportions and threatens to become a global health scourge, currently accounting for an estimated 5% of global deaths.¹ Furthermore, the World Health Organization (WHO) estimates that diabetes-related deaths 'are likely to increase by more than 50% in the next 10 years without urgent action'.¹ A co-morbidity associated with diabetes is obesity. Obesity related co-morbidities includes hypertension, dyslipidemia, coronary heart disease, stroke, some forms of cancer, musculoskeletal disorders and other cardiovascular diseases that further accelerate the morbidity and mortality associated with obesity and diabetes. Global 2005 estimates from WHO indicate that 1.6 billion adults over the age of 15 were overweight, with at least 400 million adults being obese. The fact that at least 20 million children under 5 years old are categorized as overweight foretells future health problems since 'childhood obesity is associated with a higher chance of premature death and disability in adulthood'.² Medicaments are now being prescribed to treat child-

hood obesity, as evidenced by the use of cholesterol reducing medications in this population group.³ Even though T2DM and obesity can be deterred through diet modification and increased physical exercise, pharmacologic interventions continue to be sought to treat these diseases.

A drug agent that would be expected to impact T2DM and obesity would have the potential to positively impact health outcomes for diabetics and the obese. The inhibition of acetyl-CoA carboxylase (ACC) is under investigation since modulation of its activity poses the potential to modulate diabetes and obesity.⁴ ACC is one of the enzymes responsible for modulating the rate of long chain fatty acid biosynthesis and the rate of mitochondrial fatty acid oxidation. ACC is a biotin-dependent heterodimeric protein, composed of carboxyltransferase (CT), biotin carboxy carrier protein (BCCP), and biotin carboxylase (BC) domains, whose purpose is to synthesize malonyl-CoA (m-CoA) from acetyl-CoA in an ATP-dependent reaction via the fixation of bicarbonate.⁵ The synthesis of m-CoA is a two step process wherein the first half-reaction occurs in the BC-domain and involves the ATP-dependent reaction between bicarbonate ion and enzyme-bound biotin to afford a

* Corresponding author. Tel.: +1 860 691 1687.

E-mail address: jmc1983mac@gmail.com (J.W. Corbett).

biotin-carboxylate complex. The newly formed biotin-carboxylate complex enters the CT-domain via a narrow channel between the CT- and BC-domains, where carbon dioxide is transferred from biotin carboxylate to acetyl-CoA to form m-CoA. Malonyl-CoA is then utilized by other enzymes as the substrate for de novo fatty acid synthesis and fatty acid chain elongation as well as being used as an allosteric inhibitor of carnitine palmitoyltransferase (CPT1), thereby playing a role in modulating fatty acid oxidation.

Two isoforms of mammalian ACC are known, ACC1 and ACC2 (also known as ACC α and ACC β , respectively). ACC1 is a cytosolic enzyme that produces m-CoA that is believed to be utilized in de novo fatty acid synthesis and fatty acid chain elongation while ACC2 is associated with the mitochondrial outer membrane where it may play a predominate role in producing m-CoA that functions to regulate fatty acid oxidation via allosteric inhibition of CPT1. ACC1 is found primarily in lipogenic tissues such as the liver and adipose tissue whereas ACC2 is the predominate form found in oxidative tissues (skeletal muscle and heart) where it plays a role in modulating energy expenditure. Therefore, an ACC1/2 isozyme non-selective inhibitor would be predicted to reduce fatty acid synthesis in liver and adipose tissue while at the same time increasing fatty acid oxidation in the liver and muscle tissues resulting in increased energy expenditure, decreased whole body adiposity, concomitant decreased weight gain and/or weight loss, and improved insulin sensitivity.

Screening of the Pfizer compound file and triage of the resulting hits resulted in the identification of the micromolar screening hit **1** (rACC1 IC₅₀ = 8910 nM, Fig. 1). Modeling of **1** suggested that it was binding to the same CT-domain binding channel as the historic series of ACC inhibitors, characterized by CP-640186.^{6,7} The hypothesis was made that if compound **1** had a similar binding pose as CP-640186, then the corresponding anthracene and 2-phenylquinoline amide derivatives **2** and **3** would be more potent ACC1 inhibitors since these groups led to improved potency in the CP-640186 series of ACC inhibitors. This was indeed the case as evidenced by rACC1 IC₅₀ = 325 and 842 nM for **2** and **3**, respectively. CT-domain co-crystal structures of these compounds confirmed the proposed binding mode.⁸ The crystal structure of compound **2** (in blue) is shown in Figure 2 along with an overlay of CP-640186 (in yellow, extracted from Tong's crystal structure),⁷ showing that both compounds are capable of binding to the same channel within the CT-domain. The crystal structures indicate that the anthracene rings in CP-640186 and **2** occupy a similar region of space, the morpholinyl-amide of CP-640186 is in approximately the same region of space as the methylquinoline and the H-bond between the amide carbonyl and Glu-B2026 is conserved between both compounds.

Owing to the sub-optimal physicochemical properties of the arylquinoline and anthracene amides, the chemistry team focused

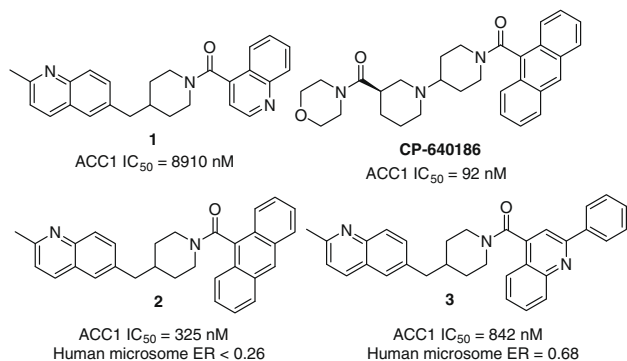


Figure 1. Structure of HTS hit **1**, CP-640186 and select analogs.

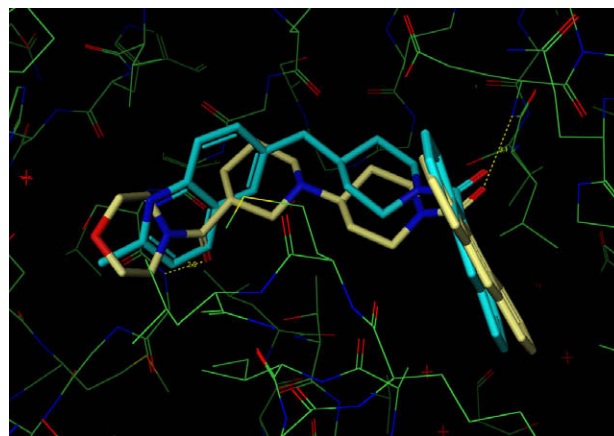


Figure 2. CT-domain co-crystal structure of **2** (blue) and CP-640186 (yellow).

on improving inhibitory potency without reverting to these functional groups. Toward that end, a carboxylic acid scan was conducted on the methylquinoline template and multiple non-arylquinoline derivatives with rACC1 IC₅₀ < 5 μ M were identified (Table 1). Compound **4** was one of the most ligand efficient (LE) inhibitors identified, with a LE of 0.26 and rACC1 IC₅₀ = 3.38 μ M.⁹ Other compounds found during the scan were *m*-substituted aryl derivatives, such as pyrazoles **5** and **6**.

Compounds **4** and **6** were submitted for rat PK and the data are summarized in Table 2. The team was encouraged by modest oral bioavailability (fraction absorbed >100%) and half-life achieved with the methylquinoline-indazole **4**. However, additional SAR on the quinoline template failed to afford needed increases in potency and it became apparent that the current template was unlikely to afford sub-micromolar potency without resorting to arylquinoline carboxylic acids.

The inability to advance the quinoline-series SAR without resorting to undesirable carboxylic acids resulted in the need to identify an alternate chemotype. The yeast CT-domain co-crystal structures of compounds **2** and **3** were subsequently used as the basis for structure-based drug design. Crystal structure of derivatives **2** and **3** showed a single H-bond interaction between the protein and ligand, namely a hydrogen-bond between the amide

Table 1

Selected data from carboxylic acid scan on methylquinoline template

Compd	Ar	rACC1 IC ₅₀ , nM ¹⁰	rACC1 LE ^a
4		3380	0.26
5		1270	0.26
6		3010	0.24

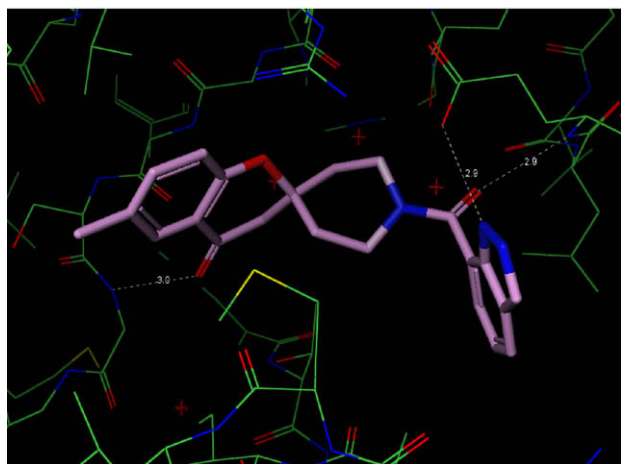
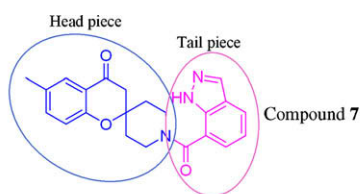
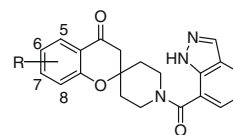
^a LE is ligand efficiency (LE = −1.4 log IC₅₀/number of heavy atoms).

Table 2
Rat PK for selected methylquinolines

	Compd 4	Compd 6
IV dose (1 mg/kg)		
CL (mL/min/kg)	44.3	34.1
Vdss (L/kg)	2.4	2.8
PO dose (5 mg/kg)		
C _{max} (ng/mL)	617	91.5
%F	45%	7–23%
t _{1/2} (h)	1.7	1.8

carbonyl and Glu-B2026. The X-ray structure of **CP-640186** indicated that Gly-B1958 could serve as an additional hydrogen-bond donor (see Fig. 2).⁷ Therefore, an effort was undertaken to utilize the methylquinoline template as a basis for creating de novo designed templates that would be expected to make additional hydrogen-bond interactions, while also reducing the degrees of freedom present in the HTS series and thereby reduce entropic penalties for binding to the enzyme.

One of the first templates modeled was the spirochromanone system. This ring system was utilized because it was more rigid and modeling suggested that it had the possibility of making additional hydrogen-bond interaction, namely one between the ketone and the protein.¹¹ A 6-methylspirochromanone was first coupled to the indazole carboxylic acid present in methylquinoline derivative **4** to provide **7**, which had an rACC1 IC₅₀ = 633 nM (Fig. 3). Gratifyingly, a yeast CT-domain co-crystal structure of **7** was obtained where it was found that three H-bonds were formed, namely the conserved amide-Glu-B2026 interaction, one between the ketone carbonyl-Gly-B1958, as in **CP-640186**, and a new interaction between indazole NH and the carboxylate of Glu-B2026 (Fig. 3).¹² The benefit, if any, arising from the indazole NH-Glu-B2026 interaction was deemed to be minimal owing to the breakage of an internal hydrogen-bond between Glu-B2026 and Arg-B1954. The ligand efficiency improvement observed with **7** compared to **4** (LE = 0.30 vs 0.26, respectively), in conjunction with its sub-micromolar potency resulted in the team focusing our synthetic efforts on this template.

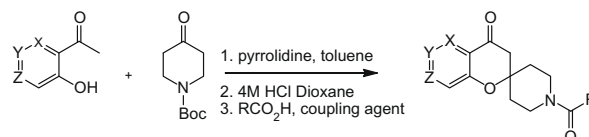
**Figure 3.** X-ray co-crystal structure of yeast CT-domain and spirochromanone **7**.**Table 3**
Initial SAR of spirochromanone system

Compd	R	rACC1 IC ₅₀ , nM	hACC2 IC ₅₀ , nM ¹⁴	rACC1 LE
8	6,7-CH ₃	163	400	0.32
7	6-CH ₃	634	641	0.30
9	7-CH ₃	850	ND ^a	0.30
10	6-MeO	562	ND ^a	0.29
11	6-Cl	1390	2130	0.29
12	6,8-CH ₃	1320	>1000	0.28
13	5-MeO	1620	>1000	0.27
14	5-MeO-6-Cl	1830	ND ^a	0.26
15	7-MeO	2530	ND ^a	0.26
16	7-Phenyl	2210	ND ^a	0.23

^a ND means no data.

Having identified a template with improved LE and having multiple hydrogen-bond interactions with the protein, the 7-indazole carboxylic acid was held constant and an initial scan of spirochromanones was undertaken (Table 3). In order to access these compounds a flexible synthetic route was developed. Base-catalyzed spirocyclization reactions of 2-acetyl-3-hydroxy-aryl and -heteroaryl compounds with boc-protected 4-piperidone afforded the desired spirochromanone systems which were then deprotected and coupled with acids under standard conditions (Fig. 4).

The most potent analog from this work was dimethyl derivative **8** (rACC1 IC₅₀ = 163 nM), which exhibited slightly improved potency relative to mono-methyl derivative **7**. Placing the methyl group in the 7-position resulted in a compound of equivalent potency as the 6-methyl derivative (compare **9** and **7**), and both are modestly lower potency and efficiency than the 6,7-dimethyl derivative **8**. The 6,8-dimethyl derivative **12** was the least potent of the methylspirochromanone derivatives, exhibiting an IC₅₀ = 1.32 μM, suggesting that substitution in the 8-position is deleterious to activity. Of the three positional isomeric methoxy derivatives prepared (**10**, **13**, and **15**), the 6-methoxy derivative **10** exhibited the best potency. Derivatization of the 6-position with a chlorine afforded compound **11** having decreased potency compared to 6-methyl derivative **8**. Interestingly, SAR was not always additive, as was evident by 5-methoxy-6-chloro derivative **14** being less active than either of the mono-substituted compounds **11** or **13**. Placement of a phenyl group in the 6-position resulted in a 3.5-fold decrease in potency compared to the 6-methyl derivative **7** (rACC1 IC₅₀ = 2210 and 633 nM for **16** and **7**, respectively). Continuing to follow LE proved useful in comparison of compounds. Compounds **15** and **16**, for example, were roughly equipotent in their ACC1 activity, but **16** was less efficient and this helped to focus the SAR development away from the 7-position. Confirmation of hACC2 activity was determined by testing select analogs and these compounds were determined to be isozyme non-selective. Significant sequence homology (>97%) exists between rat and human ACC1,¹³ therefore due to availability, purified rat ACC1 was utilized in our early screening efforts.⁶

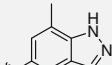
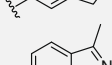
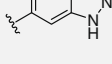
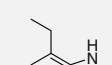
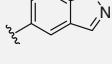
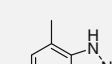
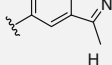
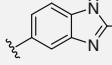
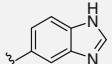
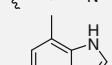
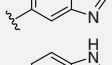
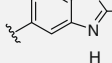
**Figure 4.** General synthetic scheme for the preparation of spirochromanone analogs.

An extensive evaluation of carboxylic acids was undertaken in an effort to identify compounds of increased potency and selected results are shown in Table 4. The 6,7-dimethyl spirochromanone was the most potent and efficient analog and this fragment was chosen for further elaboration. Since the 5-methoxy-spirochromanone probed a different vector than the 6,7-dimethyl scaffold, it was also utilized in this effort. The use of 5-carboxyindazole acids were found to consistently afford derivatives with rACC1 potency below ~100 nM. 5-Carboxybenzimidazole derivatives were generally less potent than the indazole analogs, with the exception of compound **24**, which exhibited sub-40 nM potency against both ACC isozymes.

Placement of an amide in the 2-position of the benzimidazole tail-piece, as in **24**, was well tolerated as evidenced by its inhibitory potency and an improved LE compared to benzimidazole analogs **25–27**. Therefore, a series of benzimidazole and indole analogs were made in order to more fully develop the emerging tail-piece SAR and this data is summarized in Table 5. 2-Amidobenzimidazole **24**, indole analogs **29–30** and phenyl derivative **31** suffered from modest solubility. Therefore, heterocyclic analogs **32–36** were prepared in an effort to maintain ACC inhibitory potency while attempting to improve overall solubility properties.




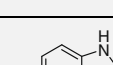
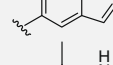
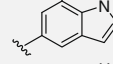
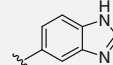
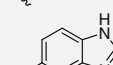
Attention was devoted to expansion of arylspiroketone SAR in an effort to identify more soluble derivatives. In particular, a vari-

Table 4
Expansion of tail-piece spirochromanone SAR

Compd	Ar	R	rACC1 IC ₅₀ (nM)	hACC2 IC ₅₀ (nM)	rACC1 LE
17		6,7-Dimethyl	22	48	0.34
18		5-MeO	104	6.5	0.32
19		6,7-Dimethyl	36	ND ^a	0.34
20		5-MeO	220	164	0.30
21		6,7-Dimethyl	17.5	ND ^a	0.34
22		5-MeO	102	151	0.31
23		5-MeO	42	11	0.32
24		5-MeO	35	16	0.32
25		5-MeO	216	111	0.31
26		5-MeO	172	126	0.31
27		5-MeO	663	>1000	0.28
28		5-MeO	2970	505	0.26

^a ND means no data.

Table 5
SAR of 5-methoxyspirochromanones

Compd	Ar	rACC1 IC ₅₀ (nM)	hACC2 IC ₅₀ (nM)	rACC1 LE
29		43	11	0.30
30		65	16	0.30
31		16	16	0.30
32		26	12	0.29
33		26	19	0.30
34		60	51	0.28
35		101	ND ^a	0.27
36		19	ND ^a	0.30

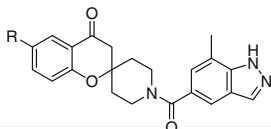
^a ND means no data.

ety of 6-substituted phenylspirochromanones were prepared (Table 6). Interestingly, it was found that the binding pocket was tolerant of polar functionality in the 6-position, as evidenced by the modest potency exhibited by carboxylic acid derivative **37** (rACC1 IC₅₀ = 303 nM). Substantial improvements in ACC potency could be achieved by building out in the vector delineated by substitution at the 6-position of the phenylspiroketone ring. Incorporation of either a pyrazole or an *N*-methylpyrazole in the 6-position provided analogs with sub-10 nM rACC1 potency (e.g., compounds **38** and **39**). The pyrazole derivatives **40** and **41** had sub-10 nM potency against hACC2 while their rACC1 activity was decreased ~2–4-fold compared to pyrazole isomers **38** and **39**, respectively. The potent ACC inhibitory activity of analogs **43–45** indicated that it was possible to place additional heterocycles into the 6-position.

Chemistry efforts were then directed at identifying a molecule with a similar ACC inhibitory profile but with decreased molecular weight. To wit, the incorporation of two of the better tail-pieces into the 7-azaspirochromanone template afforded analogs **46–48** (Table 7), with the more potent analog being *N*-methylpyrazole derivative **47**.

5-Azaspirochromanone derivatives **49–53** in Table 8 were prepared, but all compounds exhibited weak rACC1 inhibitory potency. In contrast, the 6-aza-5-alkoxyspirochromanones **54–59** had rACC1 and hACC2 IC₅₀'s below 100 nM for all prepared analogs (Table 8). Compounds having a 5-isopropoxy group were found to be the most potent ACC inhibitors (see **54** and **59**).

Compound **59** was ultimately selected for additional evaluation owing to its balanced rACC1/hACC2 inhibitory profile.¹⁵ Rat and beagle dog pharmacokinetic data for compound **59** is provided in Table 9. The compound exhibited moderate clearance in rat

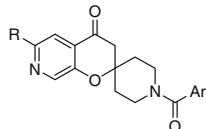
Table 6
Summary of 6-substituted phenylspiroketone SAR


Compd	R	rACC1 IC ₅₀ (nM)	hACC2 IC ₅₀ (nM)	rACC1 LE
37	CO ₂ H	303	ND ^a	0.29
38		7.4	ND ^a	0.34
39		7.5	ND ^a	0.33
40		18	4.5	0.32
41		31	6.1	0.30
42		18	7.6	0.31
43		19	30	0.31
44		17	39	0.31
45		13	6.4	0.31

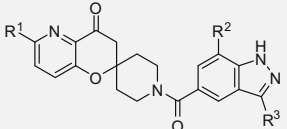
^a ND means no data.

(CL = 31 mL/min/kg) and low clearance in dog (3.6 mL/min/kg). The rat oral absorption was low-to-moderate in a methylcellulose formulation. A lipid emulsion formulation was tried resulting in decreased drug exposure, perhaps with poor drug exposure attributable to slow diffusion of drug out of the lipid droplets. It was found that a spray-dried dispersion (SDD) formulation improved the oral bioavailability (52%) indicating that this compound exhibited solubility limited absorption.

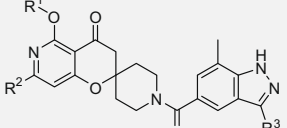
The strategy of identifying a compound with polarity in the arylchromanone ring in order to identify an analog with reasonable solubility properties, while maintaining potency at rACC1 and hACC2, afforded compound **59**. This 6-azaspiroketone derivative possessed favorable in vitro attributes and exhibited reasonable pharmacokinetic properties in two species, with low clearance observed in beagle dog. In summary, work continues to identify isozyme non-selective rACC1/hACC2 inhibitors that are highly orally bioavailable.

Table 7
SAR of azaspirochromanones


Compd	R-Group(s)	Ar	rACC1 IC ₅₀ (nM)	rACC1 LE
46			975	0.21
47			24.6	0.30
48	MeO		182	0.31

Table 8
SAR of 5- and 6-azaspirochromanones


Compd	R ₁ /R ₂ /R ₃	rACC1 IC ₅₀ (nM)	hACC2 IC ₅₀ (nM)	rACC1 LE
49	H/Me/H	154	ND ^a	0.33
50	H/Me/Me	249	363	0.31
51	Me/Me/H	366	ND ^a	0.30
52	H/H/Me	766	640	0.30
53	H ₂ N/Me/H	1350	ND ^a	0.28



54	iPr/H/H	30	4.5	0.32
55	Me/Me/H	34	48	0.33
56	iBu/H/H	23	98	0.32
57	Me/H/H	86	ND ^a	0.32
58	Et/H/H	61	ND ^a	0.32
59	iPr/H/Me	12	20	0.33

^a ND means no data.**Table 9**
Pharmacokinetic data for compound **59**.

Formulation	Rat pharmacokinetic parameters ^a				
	t _{1/2} ^b	CL ^b	Vdss ^b	%F	C _{max} , po ^a
Methylcellulose	1.4 ± 0.2	31 ± 5	3.3 ± 0.2	32 ± 5	79 ± 19
Lipid emulsion				8 ± 0	13 ± 2
Spray-dried dispersion				52 ± 9	63 ± 21
Male Beagle Dog Pharmacokinetic Data ^a					
40% PEG400/60% glycerol	6.1 ± 0.5	3.6 ± 0.4	1.6 ± 0	ND ^c	ND ^c

^a iv dose = 1 mg/kg and po dose = 3 mg/kg.^b t_{1/2} in h, CL in mL/min/kg, Vdss in L/kg.^c ND means no data.

Acknowledgment

The authors thank Bernard Fermini and Shuya Wang for hERG patch clamp studies.

References and notes

- Data was obtained from the World Health Organization website: <http://www.who.int/diabetes/en/>.
- From WHO's website: <http://www.who.int/mediacentre/factsheets/fs311/en/index.html>.
- For instance, see the guidelines for management of hyperlipidemia in children and adolescents put forward by the Kansas City Quality Improvement Consortium: <http://kcqic.org/wp-content/uploads/2008/05/2007%20KCQIC%20Hyperlipidemia%20Guideline%20Children%20and%20Adolescents.pdf>.
- For recent reviews discussing acetyl-CoA carboxylase as a potential drug target, see: (a) Harwood, H. J., Jr. *Expert Opin. Cardiovasc. Renal* **2005**, 9, 267; (b) Tong, L., ; Harwood, H. J., Jr. *J. Cell. Biochem.* **2006**, 99, 1476; (c) Corbett, J. W.; Harwood, H. J., Jr. *Recent Patents Cardiovasc. Drug Disc.* **2007**, 2, 162.
- Polakis, S. E.; Guchhait, R. B.; Zwergel, E. S.; Lane, M. D.; Cooper, T. G. *J. Biol. Chem.* **1974**, 249, 6657.
- Harwood, H. J., Jr.; Petras, S. F.; Shelly, L. D.; Zaccaro, L. M.; Perry, D. A.; Makowski, M. R.; Hargrove, D. M.; Martin, K. A.; Tracey, W. R.; Chapman, J. G.; Magee, W. P.; Dalvie, D. K.; Soliman, V. F.; Martin, W. H.; Mularski, C. J.; Eisenbeis, S. A. *J. Biol. Chem.* **2003**, 278, 37099.
- For the yeast CT-domain co-crystal structure with **CP-640186**, see: Zhang, H.; Tweel, B.; Li, J.; Tong, L. *Structure* **2004**, 12, 1683.

8. Vajdos, F.; Rajamohan, F.; Marr, E.; Corbett, J. W., in preparation.
9. Hopkins, A. L.; Groom, C. R.; Alex, A. *Drug Discovery Today* **2004**, 9, 430.
10. Rat ACC1 was obtained from rat liver based upon standard procedures such as those described by Thampy, K. G.; Wakil, S. J. *J. Biol. Chem.* **1985**, 260, 6318. The assay was conducted as described in Ref. 6.
11. Subsequent to the initiation of our work, the following patent applications published: (a) JP 2005119987; (b) WO 2007011809; (c) WO 2007011811.
12. Ascension numbers for the crystal structures are: compound **2** = 3h0j and compound **7** = 3h0s.
13. Abu-Elheiga, L.; Jayakumar, A.; Baldini, A.; Chirala, S.; Wakil, S. *Proc. Natl. Acad. Sci. U.S.A.* **1995**, 92, 4011.
14. Human ACC2 inhibition is measured using purified recombinant human ACC2 (hACC2). A full length Cytomax clone of hACC2 was purchased from Cambridge Bioscience Limited and was sequenced and subcloned into pCDNA5 FRT TO-TOPO (Invitrogen, Carlsbad, CA). The hACC2 was expressed in CHO cells by tetracycline induction and harvested in 5 L of DMEM/F12 with glutamine, biotin, hygromycin and blasticidin with 1 µg/mL tetracycline. The conditioned medium containing hACC2 was then applied to a Softlink Soft Release Avidin column (Promega, Madison, WI) and eluted with 5 mM biotin. hACC2 (4 mg) was eluted at a concentration of 0.05 mg/mL with an estimated purity of 95%. The purified hACC2 was dialyzed in 50 mM Tris, 200 mM NaCl, 4 mM DTT, 2 mM EDTA, and 5% glycerol. The pooled protein was frozen and stored at –80 °C, with no loss of activity upon thawing. For measurement of hACC2 activity and assessment of hACC2 inhibition, test compounds are dissolved in DMSO and added to the hACC2 enzyme as a 5× stock with a final DMSO concentration of 1%. rhACC2 was assayed in a Costar #3767 (Costar, Cambridge, MA) 384-well plate using the Transcreener ADP detection FP assay kit (Bellbrook Labs, Madison, WI) using the manufacturers' conditions for a 50 µM ATP reaction. The final conditions for the assay are 50 mM HEPES, pH 7.5, 5 mM MgCl₂, 5 mM tripotassium citrate, 2 mM DTT, 0.5 mg/mL BSA, 30 µM acetyl-CoA, 50 µM ATP, and 8 mM KHCO₃. Typically, a 10 µL reaction is run for 1 h at room temperature and 10 µL of Transcreener stop and detect buffer is added and incubated for an additional 1 h. The data is acquired on an Envision Fluorescence reader (Perkin Elmer) using a 620 excitation Cy5 FP general dual mirror, 620 excitation Cy5 FP filter, 688 emission (S) and a 688 (P) emission filter.
15. *Spectral data for compound 59*: LC/MS analysis Waters C18 column, 2.5 mL/min flow rate, gradient 5% ACN/95% water to 95% ACN/5% water over 3 min. LC RT 2.2 min, ESI(+) 449.4, ESI(–) 447.3. Diagnostic ¹H NMR signals (DMSO-*d*₆): 12.9 (s, 1H), 8.1 (d, *J* = 5.8 Hz, 1H), 7.6 (s, 1H), 7.2 (s, 1H), 6.7 (d, *J* = 5.9 Hz), 5.4 (m, 1H), 2.8 (s, 2H), 1.3 (d, *J* = 6.2 Hz, 6H).